

## SHOCK SYNTHESIS OF NICKEL - ALUMINIDES

A. J. Strutt, K. S. Vecchio, L. -H. Yu, M. A. Meyers and R. A. Graham †

Dept. of AMES, UC San Diego, La Jolla, CA 92093

† Sandia National Laboratory, Albuquerque, NM 87185

Chemical reactions between nickel and aluminum powder mixtures have been initiated by explosively generated high-pressure shock waves in an attempt to form Ni-Al compounds at temperatures lower than those necessary for conventional alloying. Nickel in the form of powders of "coarse"  $\sim 50\ \mu\text{m}$ , "fine"  $\sim 5\ \mu\text{m}$  and "flaky"  $\sim 40\ \mu\text{m}$  were each reacted with  $\sim 15\ \mu\text{m}$  aluminum powder at shock pressures of 7.5 and 16 GPa, in the ratio of  $3\text{Ni} + 1\text{Al}$ . Evidence of reactions leading to the formation of Ni-Al alloy phases was observed in a specimen after processing at the higher shock energy, but only in the case of "flaky" nickel. Scanning electron microscopy (SEM) of this specimen revealed regions consisting of unreacted Ni and Al particles together with isolated regions of a Ni-Al dendritic structure in the prior-Al areas. Quantitative energy-dispersive X-ray spectroscopy (EDX) of the reaction phase showed this to be  $\text{Al}_3\text{Ni}$ , while the dendritic morphology of the structure indicated that the reaction had proceeded in the liquid state.

### INTRODUCTION

The high creep resistance of many intermetallic compounds has led to many earlier studies of their high temperature mechanical properties [1-3].

In the Al-Ni system, two phases -  $\text{Ni}_3\text{Al}$  and  $\text{NiAl}$  are particularly suitable for elevated temperature applications due to relatively high melting temperatures of  $1395^\circ\text{C}$  and  $1638^\circ\text{C}$  respectively (Fig.1).

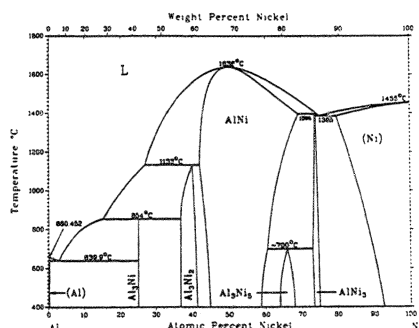


Fig.1 Al-Ni phase diagram [4].

The production of intermetallic compounds by shock induced reaction synthesis (SRS) may be achieved at lower temperatures than those involved in self-propagating high-temperature synthesis (SHS) [5] and as a result, a greater degree of control may be exercised over grain

size of the product material. Unlike SHS, SRS need not necessarily involve complete melting of reactants. Reactions may proceed as a result of the high velocity shock wave causing plastic flow and cleansing of particle surfaces [6], with additional heat provided by friction and the exothermic nature of the reaction.

Recent investigations by other workers have shown that in the shock synthesis of Ni-Al powders, the extent of the chemical reaction, and hence the products formed, depended not only on shock energy, but also on powder particle size and morphology [6,7]. However, there is still some uncertainty concerning the mechanism of the initial stages of the reaction. In the current investigation the extent of reaction was deliberately controlled so that the products of early stages of the reaction could be characterized.

### EXPERIMENTAL

Aluminum powder with spherical, 10-20  $\mu\text{m}$  sized grains was reacted with Ni powders of sizes and morphologies as shown in Table 1. (all reactants obtained from Aesar-Johnson Matthey).

All powder mixtures were in the ratio of  $3\text{Ni}:1\text{Al}$  and were shock loaded using the Sandia 'Mamma Bear' type fixture shown in Fig.2 with Baratol high explosive and under the pressure and temperature conditions outlined in Table 2.

Shock energy	Ni powder morphology and particle size	Specimen Identification
7.5 GPa	Flaky, 44 $\mu\text{m}$	2H896
	Spherical, 45-70 $\mu\text{m}$	4H896
16 GPa	Flaky, 44 $\mu\text{m}$	1H896
	Spherical, 3-7 $\mu\text{m}$	3H896

Table 1. Details of powder particle sizes, morphologies and shock pressures.

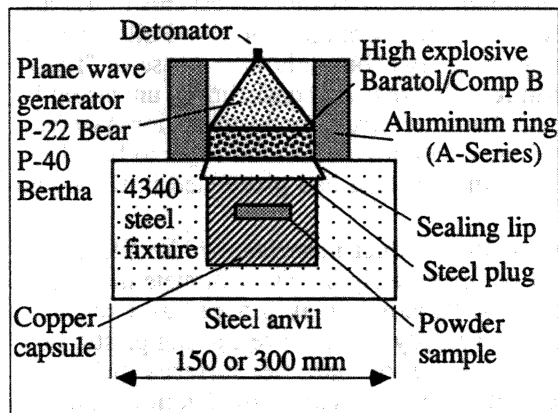


Fig. 2 Schematic representation of the Sandia Momma Bear-A fixture. [8]

The distributions of temperature and shock pressure for this type of fixture have been computed and that for temperature is shown in Fig.3 [6]. (Although the profiles were calculated for Composition-B explosive, the distribution of temperature and pressure profiles is believed to be similar to those for Baratol).

Shocked specimens were examined using SEM in a Cambridge Stereoscan 360 with a backscattered electron detector and at a beam energy of 20 keV. Chemical analysis of micro-constituents in reacted specimens was performed

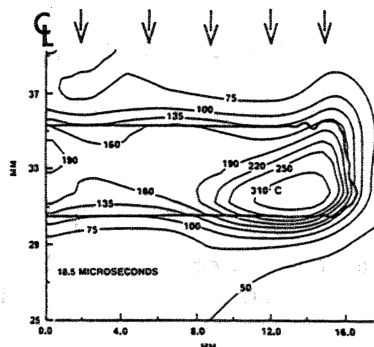


Fig. 3 Typical mean-bulk temperature distribution in powder compacts in Sandia Momma Bear A / Comp B fixture [6].

in the above microscope with the aid of a Link Systems energy-dispersive X-ray detector. Data acquired in this manner were quantified by the ratio technique [9], using a k-factor which had been derived experimentally from an  $\text{Al}_3\text{Ni}$  standard. However, corrections for the effects of selective X-ray absorption were not applied to these data.

## RESULTS

SEM micrographs of the shocked specimens are shown in Fig.4. Nickel regions appear lighter than aluminum, due to higher atomic number. In all cases, the plane of the shock wave was parallel to the long edge of the micrographs. No evidence of any reaction could be found in specimens other than in certain areas of specimen 1H896(3Ni:1Al, flaky Ni). The most widely occurring form of reaction product in 1H896 is illustrated in Fig. 5(c) and takes the form of particles of intermediate contrast (and hence of mean atomic number greater than Al, but less than Ni) which nucleate at the interface between Ni and Al and grow into the prior-Al grains.

Fixture (Baratol explosive)	Peak Pressure (GPa)		Mean Bulk Temperature, ( $^{\circ}\text{C}$ ) *	
	Bulk	Focus	Bulk	Edge
Momma Bear	$7.5 \pm 2.5$	27	225	310
Momma Bear A	$16 \pm 4.0$	32	225	310

Table 2. Characteristics of the Sandia explosive shock-loading fixtures (\*calculated temperatures are based on 50 % dense samples).

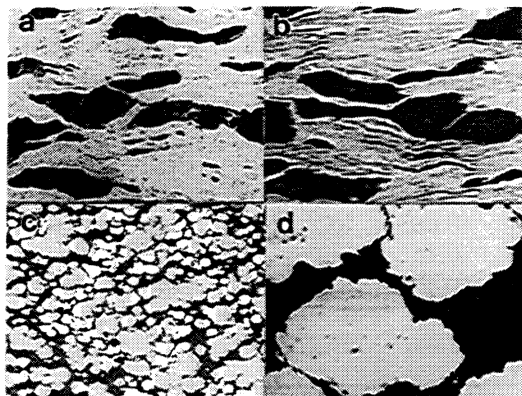


Fig. 4 Backscattered SEM images showing microstructures after shock compaction. (a) 1H896, (b) 2H896, (c) 3H896 and (d) 4H896. (x 150)

Fig. 5(b) shows Al grains typical of unreacted areas in the same specimen, which are identical to the Al-grains in a cold-compacted, un-shocked sample of flake Ni and spherical Al-powders (Fig. 5a).

In an isolated region of 1H896, an apparently more complete stage of reaction occurred, which is illustrated in Fig. 6(a). In this backscattered SEM image, the light area in the bottom right is unreacted Ni, while most of the remaining section of the micrograph shows a prior-Al region after reaction has occurred. The X-ray spectra in Fig. 6(b), (c) and (d) show qualitatively the change in Al:Ni ratio indicated in the backscattered image by the zones of different contrast. The electron interaction volume (and hence the approximate size of the region of X-ray generation) for analyses at 20 kV would be about  $1\mu\text{m}^3$  and therefore within

the boundaries of the various phase regions in Fig. 6(a).

The area represented by Fig. 6(a) was located at the bottom edge of the shock-compacted sample, and therefore in the region of highest temperature, as shown in Fig. 3. Quantification of the X-ray spectra yielded the results listed in Table 3. The first line of data corresponds to the  $\text{Al}_3\text{Ni}$  standard while the second is from the

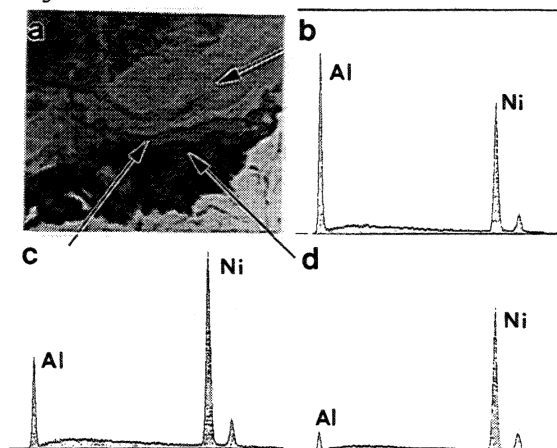


Fig. 6 (a) Backscattered SEM image of the fully-reacted region of specimen 1H896, (x 475) showing the range of reaction products of varying Al:Ni composition ratio, distinguished by varying atomic number-contrast and by the EDX spectra, (b), (c) and (d).

reaction product shown in Fig. 5(c) and is obviously  $\text{Al}_3\text{Ni}$ . The 3 EDX spectra shown in Fig. 6 (b), (c) and (d), which correspond to the zones illustrated in Fig. 6(a) and to the data on lines 4, 5 and 6 of Table 3 represent Al:Ni ratios consistent with the compositions of  $\text{Ni}_3\text{Al}$ ,  $\text{NiAl}$  and  $\text{Al}_3\text{Ni}$  respectively.

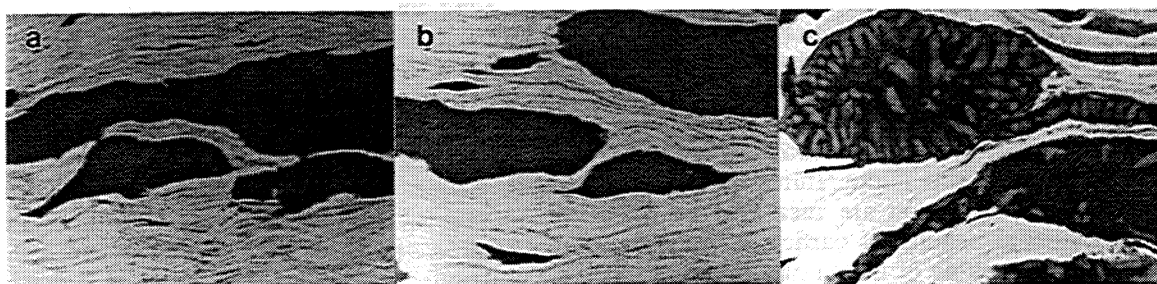


Fig. 5 Backscattered SEM micrographs showing Al-grains in specimen 1H896 before shock compaction (a) and after shock compaction: unreacted (b) and reacted (c). (x 650)

Spectrum I.D.	Description	I <sub>Al</sub> / I <sub>Ni</sub>	C <sub>Al</sub> / C <sub>Ni</sub> (weight fraction)	Al-content (wt.%) (at.%)		Theoretical Al-content (at.%)
AL3NI	Al <sub>3</sub> Ni standard	0.9	1.38	58.0	75	75
1H8961	Main reaction product in 1H	0.82	1.25	55.6	73	75
1H8962	Ni-particle	0.001	0.002	0.2	1	approx. 0 - 10
1H8963	Ni <sub>3</sub> Al reacted region	0.1	0.15	13.0	25	25 - 27
1H8964	NiAl	0.32	0.49	32.9	52	approx. 41 - 55
1H8965	Al <sub>3</sub> Ni	1.04	1.59	61.4	77	75
1H8966	Al-particle	80.05	122.48	99.2	99.5	100

Table 3. Details of quantitative EDX analyses of Al-Ni phases in specimen 1H 896.

## DISCUSSION

In Figs. 5 (c) and 6 (a), the shock-induced reaction probably occurred in the following manner. The reaction commenced at the Al / Ni interface leading to the formation of Al<sub>3</sub>Ni which grew into the prior-Al grain (in the Al<sub>3</sub>Ni+liquid 2-phase field of the phase diagram). In most regions of the specimen, temperatures were not high enough for the reaction to proceed beyond this stage. However, in the region shown in Fig. 6(a), higher temperatures were attained (and probably sustained for longer), leading to more diffusion of Ni into the Al. At this stage, the Ni-content at the original interface was higher than that required for Al<sub>3</sub>Ni, favoring the formation of Al<sub>3</sub>Ni<sub>2</sub>, and then (due to its higher exothermic energy of formation) AlNi. The final stage of the reaction at the NiAl/Ni interface was the formation of a thin layer of Ni<sub>3</sub>Al, although in the center of the prior-Al grain, insufficient Ni-diffusion occurred for the reaction to proceed beyond Al<sub>3</sub>Ni.

During the reaction, temperatures were probably above 700°C, thus preventing the formation of Al<sub>3</sub>Ni<sub>5</sub>, which was not found.

The reactions described above initiate at the Al/Ni grain boundaries due to short diffusion paths and because the temperatures attained during shock compression are increased as a result of frictional heating of particle surfaces. Although partial melting of the Al may occur (to permit the formation of Al<sub>3</sub>Ni at the Al/Ni interface) it is unlikely that sufficient temperatures could be reached to permit reaction

in the liquid state.

## REFERENCES

- [1] A. Lawley, J. A. Coll and R. W. Cahn, *Trans. AIME* **218**, pp. 166-176 (1960).
- [2] P. R. Strutt, R. S. Polvani and J. C. Ingram, *Met. Trans. A* **7A**, pp. 23-31 (1976).
- [3] J. D. Whittenberger, *J. Mater. Sci.* **22**, pp. 394-402.
- [4] M. F. Singleton, J. L. Murray and P. Nash in *Binary Alloy Phase Diagrams*, edited by T. B. Massalski, ASM, Metals Park, OH (1987) pp. 181-184.
- [5] A. N. Dremin and O. N. Bruesov, *Russ. Chem. Rev.*, **37** pp. 392-402 (1968).
- [6] N. N. Thadhani, S. Work, R. A. Graham and W. F. Hammett, *J. Mater. Res.*, **7** pp. 1063-1075 (1992).
- [7] I. Song and N. N. Thadhani, *Met. Trans. A*, **23A** pp. 41-48 (1992).
- [8] R. A. Graham and D. M. Webb in *Shock Waves in Condensed Matter 1985*, edited by Y. M. Gupta, Plenum, New York, (1986) pp. 831-836.
- [9] G. Cliff and G. W. Lorimer in *Proceedings of the 5th. European Congress on Electron Microscopy*, University of Manchester, UK, Institute of Physics, London and Bristol, (1972) pp. 140-141.